

## ORIGINAL ARTICLE

# Magnetic and optical studies on polyvinylpyrrolidone thin films doped with rare earth metal salts

Mohammad Ahmed-Fouad Basha

A casting technique was used to prepare new nanocomposite thin films of pure and  $\text{GdCl}_3$ - or  $\text{HoCl}_3$ -doped polyvinylpyrrolidone (PVP). Transmission electron microscopy (TEM) was used to study the particle size and dispersibility in the investigated nanocomposites. Magnetic measurements, using a vibrating sample magnetometer (VSM), were carried out at room temperature and applied magnetic fields up to  $10 \text{ kOe}$ . The appearance of hysteresis loops with small values of saturation flux density ( $B_s$ ), remanent flux density ( $B_r$ ), squareness ratio (SQR) and coercive field ( $H_c$ ), along with permeability ( $\mu$ ) values relatively higher than 1, may be taken, as a matter of experimentation, to consider the investigated composites as soft magnet materials. In this study, PVP- $\text{HoCl}_3$  films showed slightly better magnetic properties compared with PVP- $\text{GdCl}_3$  films. A comparative analysis of infrared (IR) and ultraviolet-visible spectra of the parent components and their composites indicated the effective role of dopant nature and concentration in morphological and microstructural changes occurring in the PVP matrix. Optical constants, such as the energy gap ( $E_g$ ) and the Urbach tail ( $E_u$ ), were determined and discussed in terms of a model based on the electronic transition between localized states in the band structure.

*Polymer Journal* (2010) 42, 728–734; doi:10.1038/pj.2010.60; published online 7 July 2010

**Keywords:** IR spectroscopy; magnetic nanocomposites; optical properties; PVP; rare earth metal salts; TEM; VSM

## INTRODUCTION

The growth in the production and use of polymers and polymeric products makes it necessary to investigate their structures, properties and the changes that take place under environmental influences. In this respect, polymeric composite systems have been a subject of both technological importance and scientific interest for a long time.<sup>1–4</sup> Doping of transition metal salts into polymers in multiphase systems can induce pronounced changes in various properties of complexes and lead to the development of materials with tailored properties.<sup>5–10</sup>

Polyvinylpyrrolidone (PVP) is a water-soluble and physiologically inert polyamide polymer. It has been attracting more and more attention because of its widespread application in the synthesis of nanostructures.<sup>11–16</sup> It exhibits unusual colloidal and complexing properties, and has been extensively used in medicine and pharmaceuticals as a protective colloid, viscosity-enhancing agent, solubility promoter, granulating/tableting agent and film-forming or coating material. Recently, it has also been used for encapsulating DNA and protecting it from intracellular degradation.<sup>13</sup>

Although numerous investigations have been conducted on a variety of polymer–metal salt systems, there is, unfortunately, nothing available in the literature, to the author's knowledge, about the physical properties of PVP doped with rare earth metal halides with an aim to characterize and understand the nature of the obtained complexes. This lack of information is mainly what dictated the choice of  $\text{GdCl}_3$  and  $\text{HoCl}_3$  as additives to the PVP matrix in this

study, in which the aim is to study the expected significant role of magnetic nanoparticles with good dispersibility in the fundamental investigations of magnetic and optical properties. Such studies are potentially promising in several practical applications.<sup>17–20</sup>

In this paper, cast films of the new composite systems PVP- $\text{GdCl}_3$  and PVP- $\text{HoCl}_3$  were prepared and subjected to comparative magnetic and optical studies using vibrating sample magnetometry (VSM), together with transmission electron microscopy (TEM) and infrared (IR) spectroscopy techniques to characterize their miscibility and complex formation. In addition, optical absorption measurements in the ultraviolet (UV)-visible region were carried out to determine the band structure and the energy gap for the samples under investigation.

## EXPERIMENTAL PROCEDURE

PVP with FW of  $\sim 40\,000$  was supplied by GFS Chemicals (Powell, OH, USA). The transition metal salts  $\text{GdCl}_3$  hydrate with FW 263.61 and  $\text{HoCl}_3 \cdot 6\text{H}_2\text{O}$  with FW 271.29 (379.38) were supplied by Strem Chemicals Inc (Newburyport, MA, USA) with purity 99.9%.

The solution method was used to obtain film samples. A known amount of PVP granules was dissolved in doubly distilled water to prepare a clear solution. In addition, a known amount of each metal salt was dissolved in a very small amount of distilled water containing a few drops of HCl at room temperature. Solutions of PVP and  $\text{GdCl}_3$  or  $\text{HoCl}_3$  were mixed together with different weight percentages (2–20 wt%), using a magnetic stirrer at  $50^\circ\text{C}$  in a water bath for several hours to obtain complete dissolution. Thin films of an

appropriate thickness (about 80  $\mu\text{m}$ ) were cast onto glass Petri dishes and then dried in air at room temperature for about 7 days, until the solvent was completely evaporated.

TEM images were taken on a Jeol JEM-1230 electron microscope (Jeol Ltd, Tokyo, Japan) at a working voltage of 100 keV. A VSM of the type VSM-9600-1 (LDI Electronics, Troy, MI, USA) was used to determine hysteresis loops for the prepared samples at room temperature and applied magnetic fields up to 8 kOe. The IR spectral analysis was performed using a PYE Unicam spectrophotometer (Pye Unicam, Cambridge, UK) over the wavenumber range of 500–4000  $\text{cm}^{-1}$ . The UV-visible absorption spectra of the samples under investigation were obtained with a Perkin-Elmer 4-B spectrophotometer (Perkin-Elmer, Waltham, MA, USA) in the wavelength range of 200–800 nm.

## RESULTS AND DISCUSSION

### TEM images

Figures 1a and b show the TEM images of the samples (a) PVP+10%  $\text{GdCl}_3$  and (b) PVP+10%  $\text{HoCl}_3$  as representatives. Statistical results revealed that the average particle sizes for samples (a) and (b) are about 33 and 18 nm, respectively. The investigated samples are nanostructured materials, and the additive salts are uniformly well dispersed in the polymeric matrix.

### Magnetic studies

Measuring the magnetism of any magnetic material vs the magnetic field at various temperatures can provide more information about the nature of the interactions of the constituent ions or groups of

molecules, as well as provide data for developing a more complete theory of magnetization.<sup>21,22</sup>

The motivation to study the magnetization of the polymeric nanocomposite systems PVP- $\text{GdCl}_3$  and PVP- $\text{HoCl}_3$  arises from a suspected connection to a category of magnetic materials, that is, magnetically hard, intermediate, soft or even superparamagnetic materials that find widespread applications in contemporary fine technologies.<sup>23,24</sup>

The characteristics of any magnetic material are best described in terms of their hysteresis loop, which gives the relationship between induction (B) or magnetization (M) and the applied magnetic field (H). The hysteresis loops of the investigated samples were measured using a VSM at room temperature and applied fields up to 10 kOe to determine magnetic parameters, such as the saturation magnetic flux density ( $B_s$ ), remanent magnetic flux density ( $B_r$ ), squareness ratio, SQR ( $B_r/B_s$ ) and coercive field ( $H_c$ ). The maximum permeability,  $\mu_{\text{max}}$ , was also determined from the B–H relations. Representative B–H loops are given in Figure 2, and the obtained results are summarized in Table 1.

A close look at Figure 2 and Table 1 indicates that the magnetic characteristics are composition dependent. As a matter of experimentation, the appearance of the hysteresis loops, even with very small values of  $B_s$ ,  $B_r$ ,  $H_c$  and SQR, along with permeability values higher than 1, may allow one to confirm a magnetically soft behavior at room temperature for the samples under investigation. Thin films of PVP- $\text{HoCl}_3$  showed comparatively better magnetic properties than the samples of PVP- $\text{GdCl}_3$ . A permeability value of 13.12 for the PVP-15 wt%  $\text{GdCl}_3$  sample was found to be the highest among all of the samples.

It should be mentioned here that the uniform distribution of permanently magnetized rare-earth nanoparticles in the PVP matrix, as illustrated by the TEM images (Figure 1), is critical in developing the experimentally established magnetic behavior for the investigated nanocomposites.<sup>25</sup>

Indeed, future studies, both experimental and theoretical, are needed to identify the various factors affecting the magnetic structure and interparticle interactions and to clarify the effects of higher and lower temperatures on the behavior of such magnetic nanocomposites.

### IR spectra

The IR spectrum is an important tool for providing information about the vibrational modes in characterizing the samples under investigation.

Figure 3 shows the IR transmittance spectra of pure  $\text{GdCl}_3$  and  $\text{HoCl}_3$  compounds in powder form and pure PVP thin films in the wavenumber range of 500–4000  $\text{cm}^{-1}$ . Both the IR spectra of pure  $\text{GdCl}_3$  and  $\text{HoCl}_3$  are characterized by the presence of the main bands assigned as  $\nu_{\text{as,s}}$  (HOH) stretching vibrations of the coordinated water at 3420 and 3390  $\text{cm}^{-1}$ ,  $\delta$  (HOH) bending vibrations of the coordinated water at 1624 and 1625  $\text{cm}^{-1}$ ,  $\gamma$  ( $\text{H}_2\text{O}$ ) at 1160 and 1021  $\text{cm}^{-1}$  and  $\omega$  ( $\text{H}_2\text{O}$ ) at 640 and 642  $\text{cm}^{-1}$  for  $\text{GdCl}_3$  and  $\text{HoCl}_3$ , respectively. The spectra show the presence of some weak sidebands and shoulders, which arise because of vibronic coupling.

The obtained results are in agreement with those recently reported in the literature for trivalent metal salts, taking into consideration that, for such compounds, the mass and size of the ion actually have an important role in determining the frequency of absorption.<sup>6,18</sup>

For the IR spectrum of pure PVP, one can easily identify peaks corresponding to the majority of the vibrational modes, despite the symmetry decrease entailed by the existence of the heteroatom and a

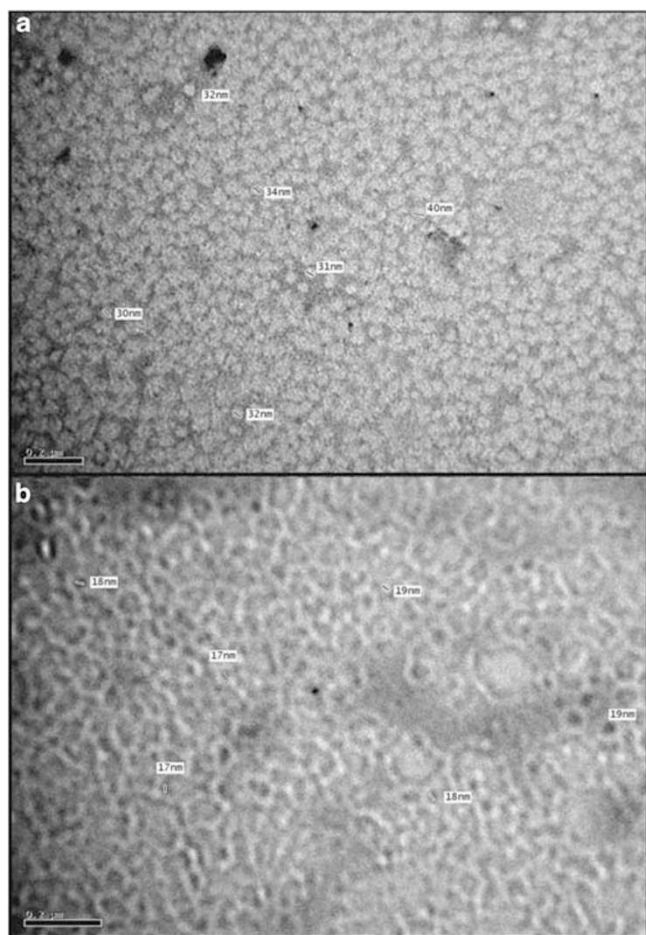


**Figure 1** TEM images of the samples: (a) PVP+10%  $\text{GdCl}_3$  and (b) PVP+ $\text{HoCl}_3$ .

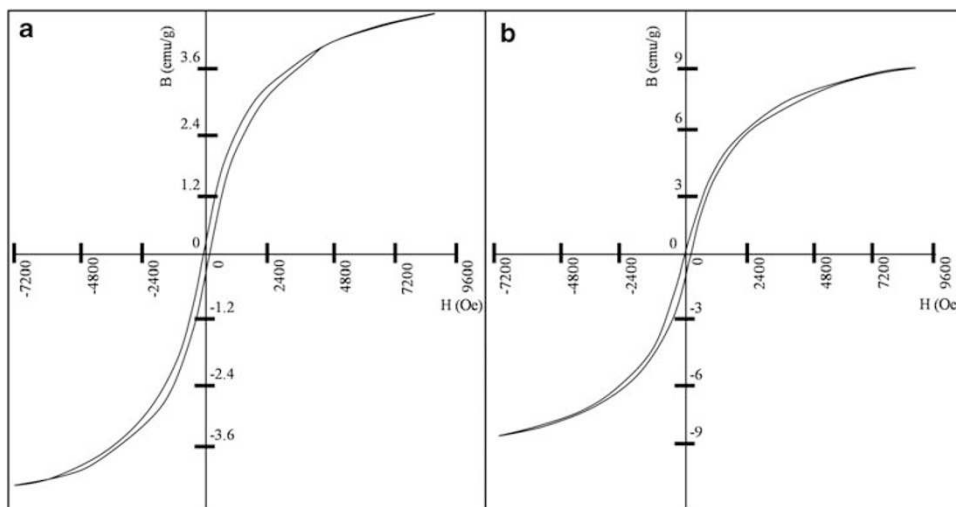


**Figure 2** Representative hysteresis B–H loops for (a) the composite film PVP+15wt% GdCl<sub>3</sub>, and (b) the composite film PVP+15wt% HoCl<sub>3</sub> at room temperature (about 27 °C).

**Table 1** The B–H curve parameters characterizing the investigated films of the nanocomposite systems PVP-GdCl<sub>3</sub> and PVP-HoCl<sub>3</sub>

Sample	$B_s$ (e.m.u. g <sup>-1</sup> )	$B_r$ (e.m.u. g <sup>-1</sup> )	$B_r/B_s$ (SQR)	$H_c$ (Oe)	$\mu_{max}$
PVP+2 wt% GdCl <sub>3</sub>	6.14	0.29	0.047	35.28	5.250
PVP+5 wt% GdCl <sub>3</sub>	6.04	0.24	0.040	39.12	5.853
PVP+10 wt% GdCl <sub>3</sub>	5.61	0.25	0.044	35.66	9.221
PVP+15 wt% GdCl <sub>3</sub>	4.72	0.26	0.045	38.71	13.12
PVP+20 wt% GdCl <sub>3</sub>	5.07	0.35	0.071	30.16	5.080
PVP+2 wt% HoCl <sub>3</sub>	7.44	0.39	0.052	35.62	4.011
PVP+5 wt% HoCl <sub>3</sub>	8.85	0.54	0.061	32.13	3.789
PVP+10 wt% HoCl <sub>3</sub>	8.45	0.42	0.050	32.15	4.882
PVP+15 wt% HoCl <sub>3</sub>	9.06	0.41	0.046	34.93	6.156
PVP+20 wt% HoCl <sub>3</sub>	7.53	0.44	0.058	31.69	3.491

Abbreviations: PVP, polyvinylpyrrolidone; SQR, squareness ratio.

carbonyl group in the pyrrolidone ring. The empirical assignments of the most evident absorption bands for the pure PVP thin film investigated in this study are consistent with those previously reported in literature.<sup>12,15,26</sup> The relatively broad  $\nu$  (OH) stretching band centered at about 3450 cm<sup>-1</sup> indicates the presence of the stretching vibration associated with free and numerous hydroxyl groups (–OH), in addition to hydrogen-bonded (HOH) due to residual water<sup>6,11</sup> because the samples were not vacuum dried. The observed characteristic band of PVP at 1675 cm<sup>-1</sup> is due to the carbonyl (C=O) stretching, which is very sensitive to hydrogen bond formation with water molecules. Taylor *et al.*<sup>27</sup> and Tanaka *et al.*<sup>28</sup> reported that the  $\nu$  (C=O) shifts from 1680 to 1652 cm<sup>-1</sup> as the concentration of adsorbed water is increased.

In addition, the distinctive doublet appearing at 2362 and 2324 cm<sup>-1</sup> and a small broad peak at 2134 cm<sup>-1</sup> are clearly evident in the obtained spectrum of pure PVP.

Figures 4A and B show the IR spectra of doped PVP thin films with 2, 5, 10, 15 and 20 wt% GdCl<sub>3</sub> or HoCl<sub>3</sub>, respectively, in the region of 500–4000 cm<sup>-1</sup>. Careful examination of these spectra showed that a gradual decrease can be generally observed in the intensity of the bands characterizing the dopant concentrations within the wavenum-

ber range of 1500–4000 cm<sup>-1</sup>. One can observe that the small broad peak of pure PVP at 2134 cm<sup>-1</sup> in Figure 3 disappeared completely in all the spectra of the composite samples containing 2, 5, 10, 15 and 20 wt% GdCl<sub>3</sub> (Figure 4A), while its disappearance was observed only in the spectra of the samples containing 15 and 20 wt% HoCl<sub>3</sub> (Figure 4B).

It is also to be noted that the intensity of the bands in the range of 500–1500 cm<sup>-1</sup> exhibited a remarkable increase for the composite film PVP-5 wt% HoCl<sub>3</sub> (Figure 4B). In contrast, all the bands in the range of 500–1230 cm<sup>-1</sup> seemed to be diminishing in the IR spectra of the PVP-GdCl<sub>3</sub> composite films (Figure 4A).

The only remarkable change in the position of the bands was that determined at the characteristic frequency of 1675 cm<sup>-1</sup> assigned to C=O stretching mode (Figure 3). This significant peak exhibited a regular decrease toward lower wavenumber (from 1675 to 1644 cm<sup>-1</sup>) with the increase of the GdCl<sub>3</sub> dopant concentration (Figure 4A) and showed less irregular decrease (from 1675 to 1655 cm<sup>-1</sup>) with the increase of HoCl<sub>3</sub> dopant concentration (Figure 4B). The intensity of this band is also composition dependent.

Koo *et al.*<sup>29</sup> attributed such a shift to lower energies in Ni nanoparticle spectra of Ni-PVP at 1661 cm<sup>-1</sup> and assigned the C=O stretching vibration to the chemical interaction between the PVP molecules and the nickel nanoparticle surface. This result represents strong evidence that this interaction occurs through the C=O groups of the PVP.<sup>29,30</sup>

In addition, Caykara *et al.*<sup>26</sup> considered a shift of about 15 cm<sup>-1</sup> to lower wavenumbers for the C=O stretching band for the PVP component in a blend with sodium alginate to be a strong support to the idea that a hydrogen bond can form between =C=O groups of the PVP and –OH groups of NaAlg. Feng *et al.*<sup>31</sup> indicated that the shifts in the IR bands for PVP in a hybrid film containing ZnO nanoparticles should be attributed to the strong coulombic interaction between ZnO and the polymeric matrix.

Furthermore, noticeable broadening can be seen for the band at about 3450 cm<sup>-1</sup> with the increase of the additive concentration. This peak shift and broadening may be taken as an indication of complexation between GdCl<sub>3</sub> or HoCl<sub>3</sub> and the PVP backbone.<sup>6</sup> It is usually accepted that the pyrrolidone group of PVP prefers to complex with many inorganic salts, resulting in fine dispersion and surface passivation.<sup>31</sup>

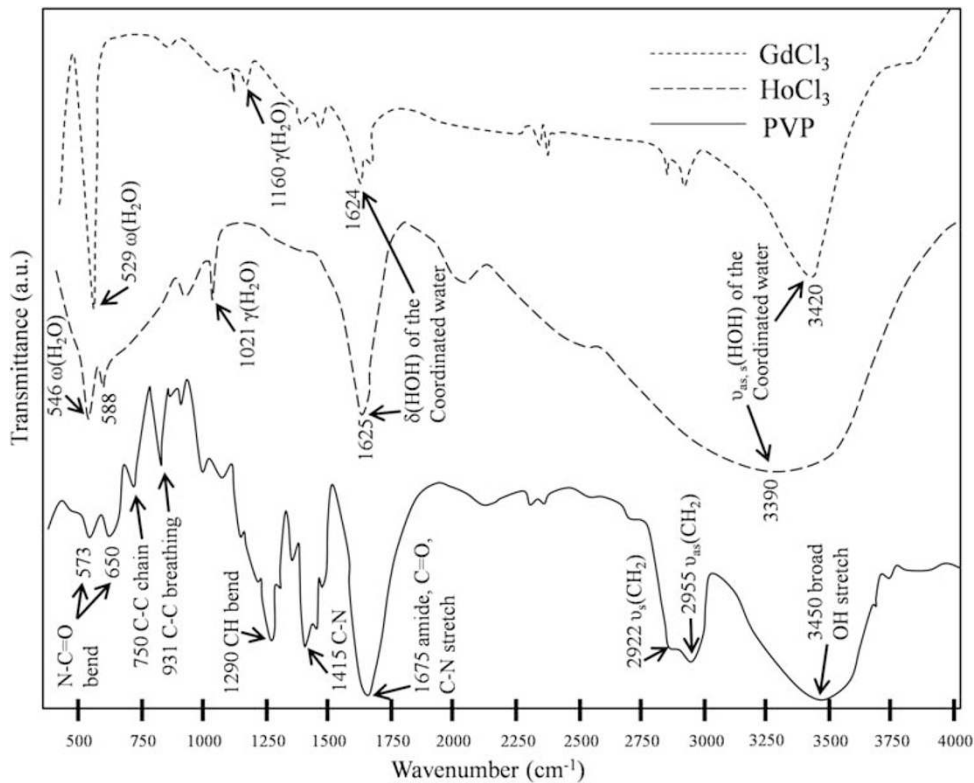


**Figure 3** IR spectra of pure  $\text{GdCl}_3$ , pure  $\text{HoCl}_3$  and pure PVP. The notation for the types of the vibrational modes:  $\gamma$ -scissoring,  $\omega$ -wagging,  $\nu_{as}$ ,  $\nu_s$ -asymmetric and symmetric stretching modes, and  $\delta$ -bending.

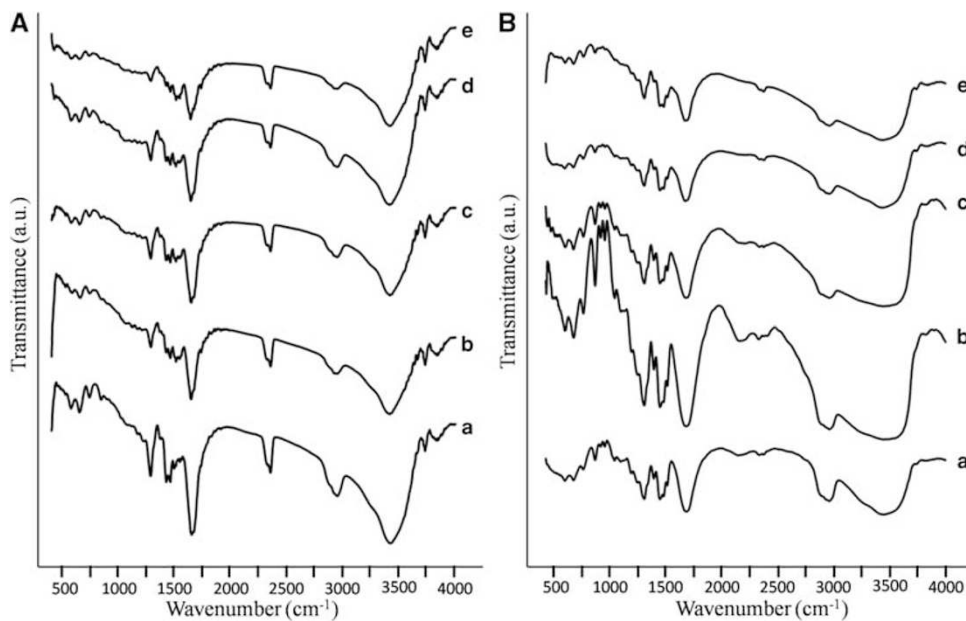


**Figure 4** IR spectra of (A) (a) 2, (b) 5, (c) 10, (d) 15 and (e) 20wt%  $\text{GdCl}_3$ -doped PVP; and (B) (a) 2, (b) 5, (c) 10, (d) 15 and (e) 20wt%  $\text{HoCl}_3$ -doped PVP.

### Optical studies

**UV-visible spectra.** Figure 5A displays the UV-visible absorbance spectra of the pure compounds  $\text{GdCl}_3$  and  $\text{HoCl}_3$  in the wavelength range of 200–800 nm.

It can be seen that the absorption spectrum of  $\text{HoCl}_3$  is more intense than that of  $\text{GdCl}_3$ , with the appearance of identical intense peaks at 220 nm in the UV region. Such absorption bands occurring in the UV region for rare earth metal salts are reasonably assigned

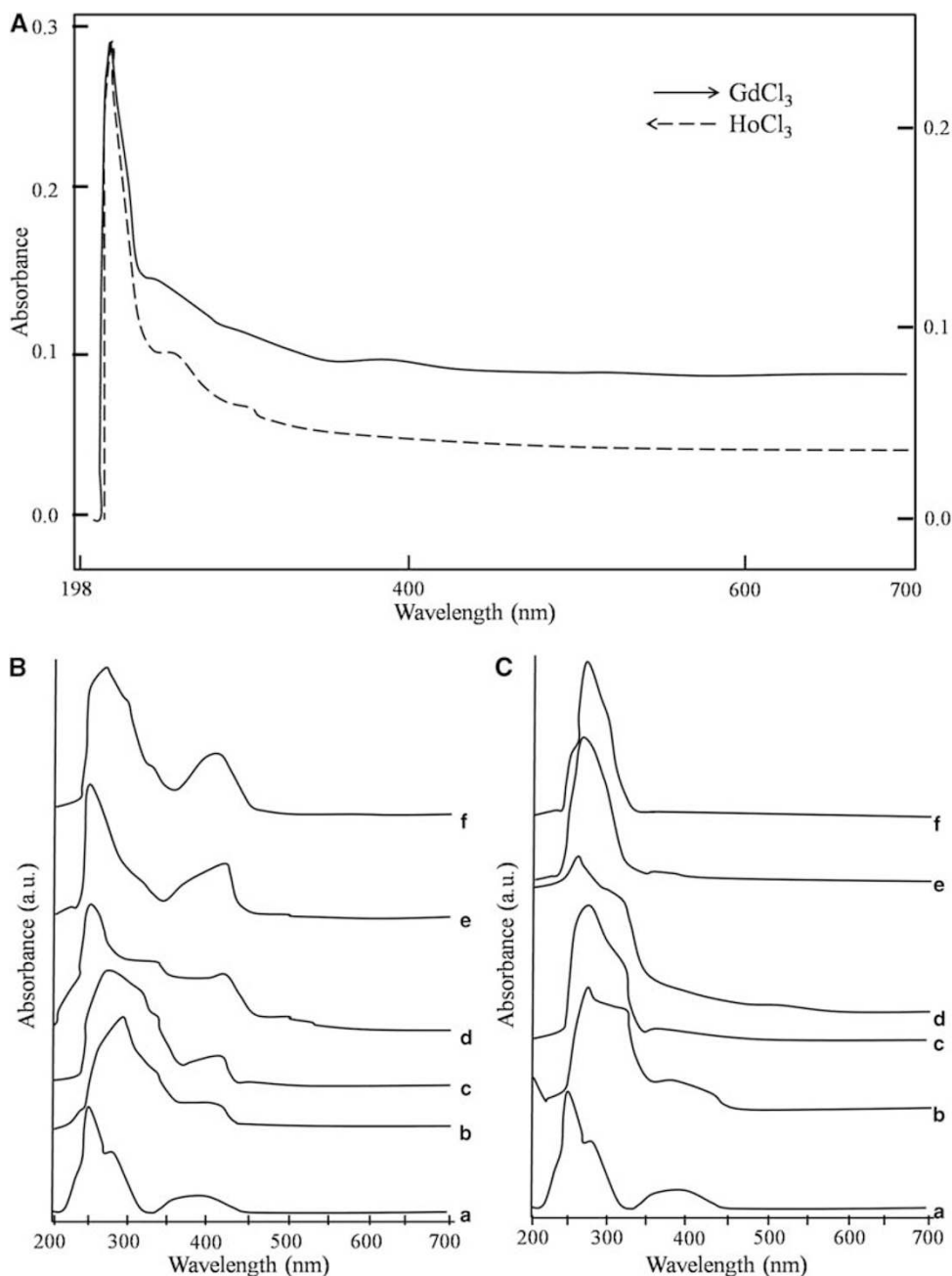


**Figure 5** UV-visible spectra of (A) pure GdCl<sub>3</sub> and HoCl<sub>3</sub> compounds; (B) (a) pure PVP, (b) 2, (c) 5, (d) 10, (e) 15 and (f) 20 wt% GdCl<sub>3</sub>-doped PVP; and (C) (a) pure PVP, (b) 2, (c) 5, (d) 10, (e) 15 and (f) 20 wt% HoCl<sub>3</sub>-doped PVP.

to the electronic transitions of the chromophoric group in their configurations.<sup>6</sup>

Figures 5B and C depict the UV-visible absorption spectra of the prepared composite systems PVP-GdCl<sub>3</sub> and PVP-HoCl<sub>3</sub>, respectively, with dopant concentrations of 2, 5, 10, 15 and 20 wt%, in the wavelength range of 200–800 nm. The spectrum (a) of pure PVP showed a sharp absorption band at 249 nm, along with a shoulder at 280 nm and an ill-defined band at 380 nm. Khare *et al.*<sup>32</sup> reported a well-defined sharp band at about 246 nm for pure PVP. Jin *et al.*<sup>13</sup> confirmed that a strong absorbance at about 225 nm for pure PVP is assigned to the carbonyl group, and a new absorbance appearing at

about 245 nm is assigned to the carbonyl group by the adjoining allyl bromide. A higher absorbance with a disappearance of the ill-band of PVP at about 380 nm for dopant concentrations of > 2 wt% HoCl<sub>3</sub> characterizes the composite films of the PVP-HoCl<sub>3</sub> system in the wavelength range of 200–800 nm.

The shoulder observed at 280 nm in the PVP spectrum was found to exhibit some development with a slight shift toward larger wavelengths, depending on the dopant concentration for PVP-HoCl<sub>3</sub> samples. In addition, the well-defined peak that appeared at 249 nm was observed to exhibit changes in shape, intensity and position for both systems. All these optical changes give further

evidence for complete miscibility between the dopants and PVP, in addition to a probable modification in molecular structure, and seem to conform with the information obtained from the TEM images, magnetic studies and IR spectroscopy.

**Optical parameters.** The absorption coefficient  $\alpha(\nu)$  at frequency  $\nu$  can be directly determined from the optical absorption spectra using the relationship:

$$\alpha = \frac{1}{d} \ln \left( \frac{1}{T} \right) \text{ or } \alpha = \frac{A}{d}, \quad (1)$$

where  $T$  is the transmittance,  $A$  is the absorbance and  $d$  is the thickness of the film. The fundamental absorption edge is one of the most important features of the absorption spectra of crystalline and amorphous materials. It was found to follow an exponential law, and the absorption coefficient  $\alpha(\nu)$  above the exponential tail has been observed to obey an equation of the form

$$\alpha(\nu) = B(\hbar\nu - E_g)^r / \hbar\nu, \quad (2)$$

where  $B$  is a constant,  $E_g$  is the optical energy gap and  $r$  is an index that can assume values of  $1/2$ ,  $3/2$ ,  $2$  and  $3$ , depending on the nature of the electronic transition responsible for the absorption.<sup>33</sup> The range of the validity of this equation is too small, and hence it becomes very difficult to determine the exact value of the exponent  $r$ .<sup>34</sup>

In this study, the fits for all values of  $r$  were compared for different compositions of the PVP-GdCl<sub>3</sub> and PVP-HoCl<sub>3</sub> films. It was found that the values  $r=2$  and  $r=1/2$  gave a better fit to the experimental results than the other exponents, suggesting the existence of both direct and indirect types of optical transition.<sup>34</sup> The value of  $E_g$  is obtained from the plots of  $(\alpha h\nu)^{1/2}$  and  $(\alpha h\nu)^2$  in the high absorption range and extrapolating the linear regions of the plots to zero absorption.

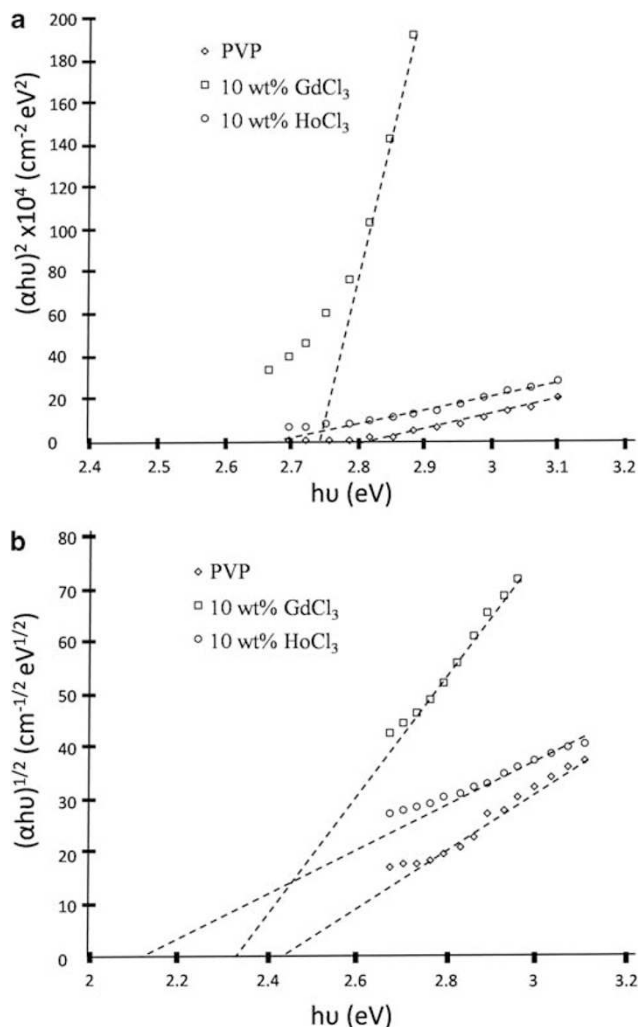
Representative plots are shown in Figure 6, and the obtained values of  $E_g$  for the investigated samples are listed in Table 2. It should be noted that the values of the direct and indirect optical band gaps depend on both the dopant type and concentration. It is clear from Table 2 that these values started to decrease on doping up to a dopant concentration of 10 wt%, then showed an increase corresponding increases in dopant concentration, probably due to segregation effects.<sup>35</sup>

Figure 7 shows representative plots between  $\ln(\alpha)$  and  $h\nu$  for pure PVP, PVP-5 wt% GdCl<sub>3</sub> and PVP-5 wt% HoCl<sub>3</sub> films. The straight lines obtained confirm the dependence of the absorption coefficient on the photon energy in accordance with the empirical Urbach formula<sup>34</sup>:

$$\alpha\nu = \alpha_0 e^{(h\nu/E_c)} \quad (3)$$

where  $\alpha_0$  is a constant and  $E_c$ , calculated from the slopes of the straight lines, has been interpreted as the width of the tails of the localized states in the forbidden gap.

It should be mentioned that an Urbach tail has been observed in both amorphous and crystalline materials. Therefore, nothing can be said with certainty about the origin of this exponential dependence.<sup>34</sup> The obtained values of Urbach  $E_c$  for all samples are shown in Table 2. It is clear that these values vary largely with composition in an irregular trend, within the range from 0.16 to 0.73 eV for PVP-GdCl<sub>3</sub> films and in the range from 0.09 to 0.52 eV for PVP-HoCl<sub>3</sub> films. Thus, a model based on the electronic transition between localized states suggests that some tail states are generated in the systems under investigation<sup>33</sup> in which the dopant concentration has an important role in morphological and microstructural changes occurring in the polymer matrix.<sup>33–35</sup>



**Figure 6** Representative plots of (a)  $(\alpha h\nu)^2$  vs  $h\nu$  for pure PVP, PVP+10wt% GdCl<sub>3</sub> and PVP+10wt% HoCl<sub>3</sub> films, and (b)  $(\alpha h\nu)^{1/2}$  vs  $h\nu$  for pure PVP, PVP+10wt% GdCl<sub>3</sub> and PVP+10wt% HoCl<sub>3</sub> films.

**Table 2** Calculated values of direct and indirect optical band gap  $E_g$  and Urbach tail  $E_c$  for PVP-GdCl<sub>3</sub> and PVP-HoCl<sub>3</sub> nanocomposite films

Sample	Optical band gap $E_g$ (eV)		Urbach tail $E_c$ (eV)
	Direct	Indirect	
PVP	2.80	2.42	0.28
PVP+2 wt% GdCl <sub>3</sub>	2.80	2.38	0.22
PVP+5 wt% GdCl <sub>3</sub>	2.76	2.35	0.41
PVP+10 wt% GdCl <sub>3</sub>	2.75	2.32	0.73
PVP+15 wt% GdCl <sub>3</sub>	2.75	2.49	0.16
PVP+20 wt% GdCl <sub>3</sub>	2.81	2.51	0.49
PVP+2 wt% HoCl <sub>3</sub>	2.73	2.35	0.09
PVP+5 wt% HoCl <sub>3</sub>	2.71	2.22	0.20
PVP+10 wt% HoCl <sub>3</sub>	2.67	2.11	0.52
PVP+15 wt% HoCl <sub>3</sub>	2.70	2.12	0.19
PVP+20 wt% HoCl <sub>3</sub>	2.72	2.13	0.37

Abbreviation: PVP, polyvinylpyrrolidone.

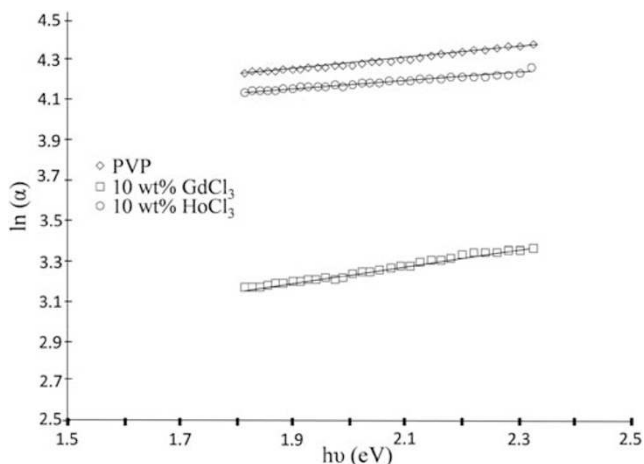


**Figure 7** Plots of  $\ln(\alpha)$  vs  $h\nu$  for pure PVP, PVP+5wt%  $\text{GdCl}_3$  and PVP+5wt%  $\text{HoCl}_3$ .

## CONCLUSION

The main results of this study are summarized as follows:

- (i) New magnetic nanocomposite thin films of the systems PVP+ $\text{GdCl}_3$  and PVP+ $\text{HoCl}_3$  have been prepared using the casting technique.
- (ii) The images obtained by using a TEM confirmed the nanostructured nature of the investigated samples and indicated the uniform distribution of the additive rare earth chlorides as nanoparticles in the PVP matrix.
- (iii) The hysteresis loops obtained using a VSM revealed that the investigated thin films behave as magnetically soft materials characterized by very small values of  $B_s$ ,  $B_r$  and  $H_c$ , along with permeability values higher than 1 at room temperature.
- (iv) The reported changes in the intensity, position and shape of the bands in the IR and UV-visible spectra depending on dopant concentration in the prepared samples confirm the miscibility and the formation of complexes between  $\text{GdCl}_3$  or  $\text{HoCl}_3$  and the PVP backbone or a probable modification in the molecular structure.
- (v) A model based on the electronic transition between localized states seemed suitable for determining the nature and width of the optical band gaps and to calculate some optical constants, such as the direct and indirect energy gap, together with the so-called Urbach tail. The three parameters are composition dependent.

- 1 Garbassi, F. in *Analysis and Characterization of Polymers* (ed. Maiti, S.) 210 pp. (Anusandahn Prakashan, Midnapore, India, 2003).
- 2 Sheldon, R. P. *Composite Polymeric Materials*, Applied Science, Elsevier Science, London and New York, 1982).
- 3 Basha, A. F., AbdelSamad, H. A. & Amin, M. Investigation of permanent polarization in poly(vinylalcohol). *Ind. J. Phys* **59A**, 213–218 (1985).
- 4 Nikolova, K., Panchev, I. & Sainov, S. Optical characteristics of biopolymer films from pectin and gelatin. *J. Optoelectron. Adv. Mater.* **7**, 3, 1439–1444 (2005).
- 5 Anantharaman, M. R., Malini, K. A., Sindhu, S., Mohammed, E. M., Date, S. K., Kulkarni, S. D., Joy, P. A. & Kurian, P. Tailoring magnetic and dielectric properties of rubber ferrite composites containing mixed ferrites. *Bull. Mater. Sci.* **24**, 6, 623–631 (2001).
- 6 Abdel Kader, F. H., Osman, W. H., Ragab, H. S., Shehap, A. M., Rizk, M. S. & Basha, M. A. F. Electrical and optical properties of polyvinyl alcohol thin films doped with metal salts. *J. Polym. Mater.* **21**, 49–60 (2004).

- 7 Faria, I. O. & Moreira, R. L. Dielectric behavior of P(VDF-TrFE)/PMMA blends. *J. Polym. Sci. B Polym. Phys.* **37**, 2996–3002 (1999).
- 8 Nagasawa, T., Murata, Y., Todono, K., Kawai, R., Kethara, K. I. & Yono, S. Dielectric properties of polyarylate blends. *J. Mater. Sci.* **35**, 3077–3082 (2000).
- 9 Kolekar, C. B., Kamble, P. N. & Vaingankar, A. S. Structural and DC electrical resistivity study of  $\text{Gd}^{3+}$ -substituted Cu-Cd mixed ferrites. *J. Magn. Magn. Mater.* **138**, 211–215 (1994).
- 10 Abdel Kader, F. H., Osman, W. H., Mahmoud, K. H. & Basha, M. A. F. Dielectric investigations and ac conductivity of polyvinyl alcohol films doped with europium and terbium chloride. *Physica B* **403**, 3473–3484 (2008).
- 11 Viau, G., Fievet-Vincnt, F. & Fievet, F. Nucleation and growth of bimetallic CoNi and FeNi monodisperse particles prepared in polyols. *Solid State Ionics* **84**, 259–270 (1996).
- 12 Kumar, V., Yang, T. & Yang, Y. Interpolymer complexation. I. Preparation and characterization of a polyvinyl acetate phthalate-polyvinylpyrrolidone (PVAP-PVP) complex. *Int. J. Pharmaceutics* **188**, 221–232 (1999).
- 13 Jin, S., Lin, M., Chen, S. & Gao, C. Synthesis, characterization and the rapid response property of the temperature responsive PVP-g-PNIPAM hydrogel. *Eur. Polym. J.* **44**, 2162–2170 (2008).
- 14 Liu, X., Han, K., Gu, M., Huang, S., Liu, B. & Ni, C. Optical properties of  $\text{GdTaO}_4:\text{Eu}^{3+}$  thick films prepared from a PVP-containing solution. *Appl. Surface Sci.* **255**, 4680–4683(2009).
- 15 Slistan-Grijalva, A., Herrera-Urbina, R., Rivas-Silva, J. F., Avalos-Borja, M., Castillon-Barraza, F. F. & Posada-Amarillas, A. Synthesis of silver nanoparticle in a polyvinylpyrrolidone (PVP) paste and their optical properties in a film and in ethylene glycol. *Mater. Research Bull.* **43**, 90–96 (2008).
- 16 Mateo-Mateo, C., Vazquez-Vazquez, C., Bujan-Munoz, M. C., Lopez-Quintela, M. A., Serantes, D., Baldomir, D. & Rivas, J. Synthesis and characterization of  $\text{CoFe}_2\text{O}_4$ -PVP nanocomposites. *J. Non-Cryst. Solids* **354**, 5236–5237 (2008).
- 17 Lu, X., Niu, M., Oiao, R. & Gao, M. Superdispersible PVP-coated  $\text{Fe}_3\text{O}_4$  nanocrystals prepared by a 'One-Pot' reaction. *J. Phys. Chem. B* **112**, 14390–14394 (2008).
- 18 Oczko, G. & Macalik, L. Optical properties of single crystals of heavy lanthanide chlorides. *Polyhedron* **29**, 1231–1236 (2010).
- 19 Su, L., Yang, L., Wang, Z., Jin, X., Weng, S., Yan, Ch., Yu, Z. & Wu, J. Crystal structures and spectroscopic characterization of galactitol complexes of trivalent lanthanide and divalent alkaline earth chlorides. *Carbohydr. Res.* **341**, 75–83 (2006).
- 20 Kovács, A., Konings, R. J. M. & Booi, A. S. High temperature infrared spectra of rare earth trihalides. Part I.  $\text{CeCl}_3$ ,  $\text{NdCl}_3$ ,  $\text{SmCl}_3$ ,  $\text{GdCl}_3$  and  $\text{DyCl}_3$ . *Vib. Spectrosc.* **10**, 65–70 (1995).
- 21 Pradeep, A., Priyadharsini, P. & Chandrasekaran, G. Sol-gel route of synthesis of nanoparticles of  $\text{MgFe}_2\text{O}_4$  and XRD, FTIR and VSM study. *J. Magn. Magn. Mater.* **320**, 2774–4779 (2008).
- 22 Roy, P. K. & Bera, J. Electromagnetic properties of samarium-substituted NiCuZn ferrite prepared by auto-combustion method. *J. Magn. Magn. Mater.* **321**, 247–251 (2009).
- 23 Andriessen, F. & Torpstra, M. (editors), *Rare Earth Metals Based Permanent Magnets*, (Elsevier Applied Science, UK, 1989).
- 24 Parker, R. J. (*Advances in Permanent Magnetism*, John Wiley & Sons, New York, 1990).
- 25 Gabal, M. A. Effect of Mg substitution on the magnetic properties of NiCuZn ferrite nanoparticles prepared through a novel method using egg white. *J. Mag. Mag. Mater.* **321**, 3144–3148 (2009).
- 26 Caykara, T., Demirci, S. & Kantoglu, O. Thermal, spectroscopic and mechanical properties of blend films of poly (*N*-vinyl-2-pyrrolidone) and sodium alginate. *Polymer-Plastics Tech. Engin.* **46**, 737–741 (2007).
- 27 Taylor, L. S., Langkilde, F. W. & Zograf, G. J. Fourier transform Raman spectroscopic study of the interaction of water vapor with amorphous polymers. *Pharm. Sci.* **90**, 888–901 (2001).
- 28 Tanaka, N., Ito, K. & Kitano, H. Raman spectroscopic study of hydrogen bonding of poly(*N*-vinyl-2-pyrrolidone) in heavy water and dimethyl sulfoxide. *Macromol. Chem. Phys.* **195**, 3369–3380 (1994).
- 29 Koo, C. M., Ham, H. T., Choi, M. H., Kim, S. O. & Chung, I. J. Characteristics of polyvinylpyrrolidone-layered silicate nanocomposites prepared by attrition ball milling. *Polymer* **44**, 681–689 (2003).
- 30 Couto, G. G., Klein, J. J., Schreiner, W. H., Mosca, D. H., de Oliveira, A. J. A. & Zarbin, A. J. G. Nickel nanoparticles obtained by a modified polyol process. Synthesis, characterization, and magnetic properties. *J. Colloid Interface Sci.* **311**, 461–468 (2007).
- 31 Feng, W., Tao, H. & Liu, Y. Structure and optical behaviour of nanocomposites hybride films of well monodispersed ZnO nanoparticles into poly (vinylpyrrolidone). *J. Mater. Sci. Technol.* **22**, 2, 230–234 (2006).
- 32 Khare, P. K., Paliwal, S. K., Kuraria, R., Vishwakarma, H. L., Verma, A. & Jain, S. K. Electrical condition mechanism in solution grown doped polyvinyl pyrrolidone films. *Bull. Mater. Sci.* **21**, 2, 139–147 (1998).
- 33 Davis, E. A. & Mott, N. F. Conduction in non-crystalline systems V. Conductivity, optical absorption and photoconductivity in amorphous semiconductors. *Phil. Mag.* **22**, 903–922 (1970).
- 34 Chopra, N., Mansingh, A. & Chadha, G. K. Electrical, optical and structural properties of amorphous  $\text{V}_2\text{O}_5\text{-TeO}_2$  blown films. *J. Non-Cryst. Solids* **126**, 194–201 (1990).
- 35 Devi, C. U., Sharma, A. K. & Rao, V.V.R.N. Electrical and optical properties of pure and silver nitrate-doped polyvinyl alcohol films. *Mater. Lett.* **56**, 167–174 (2002).